

Sanxi Li, Nan Wei and Wenzheng Zhang*

Morphology and ferroelectric properties of Ce-substituted $\text{Bi}_4\text{Ti}_3\text{O}_{12}$ thin films prepared by sol-gel method

Abstract: The Ce-substituted bismuth titanate ($\text{Bi}_4\text{Ti}_3\text{O}_{12}$) ferroelectric thin films were prepared on Pt/Ti/SiO₂/Si substrates by sol-gel method and annealed at 700°C. The Bi-layered perovskite (with Ce substitution for Bi) single phase films were obtained and the thickness was 500 nm. At 12 V amplitude and 1000 Hz frequency, ferroelectric tests results showed a hysteresis loop with remnant polarization (2Pr) and coercive field values (2Ec) of 9.86 $\mu\text{C}/\text{cm}^2$ and 208 kV/cm, respectively. The structure and lattice parameters were analyzed by X-ray diffraction (XRD). The results showed that by increasing Ce substitution the ratio of a/c, the ferroelectric properties, increased when the Ce-substitution of 0.6, a and c values were 5.40734 Å and 5.3559 Å, respectively. The a-axis highly oriented structure may have influenced the remnant polarization and coercive field values of the films obtained.

Keywords: bismuth titanate; ferroelectric; lattice parameter; sol-gel.

*Corresponding author: Wenzheng Zhang, Shenyang University of Chemical Technology, Shenyang Economic & Technology Development Zone, Shenyang, 110142, China, e-mail: zhangwenzheng_0@163.com

Sanxi Li: Materials Chemistry, Shenyang University of Chemical Technology, Shenyang Economic & Technology Development Zone, Shenyang, Liao Ning 110142, China; and College of Science, Shenyang University of Technology, Shenliao West Road, Economic & Technological Development Zone, Shenyang, 110870, China

Nan Wei: Materials Chemistry, Shenyang University of Chemical Technology, Shenyang Economic & Technology Development Zone, Shenyang, Liao Ning 110142, China

1 Introduction

Ferroelectric thin films have attracted considerable attention due to their applications in non-volatile ferroelectric random access memory (FeRAM) [1]. Lead zirconate titanate (PZT) thin films which have always been considered the best candidates for non-volatile ferroelectric random access memory were found to exhibit gradual environmental

pollution and fatigue resistance [2]. With the advantages of good ferroelectric properties [3] and fatigue resistance, lead-free bismuth-layer perovskite ferroelectric materials tend to replace the PZT. $\text{Bi}_4\text{Ti}_3\text{O}_{12}$ (BTO) were typical layered [4] perovskite ferroelectrics materials with the tendency to replace rare earth element which will improve the residual polarization value and improve the fatigue resistance. The evaporation of bismuth creates vacancy defects [5] and the defects produce $\text{Bi}_4\text{Ti}_3\text{O}_{12}$ films with high leakage of current and domain pinning, however after partial Bi is replaced by the rare earth element, the valency defects which were caused by the volatility of Bi was inhibited and the ferroelectric effect improved. The films have been prepared by sol-gel method, pulsed laser deposition (PLD), sputtering, chemical vapor deposition (CVD), molecular beam epitaxy (MBE), liquid-phase deposition (LPD), and so on [6]. The sol-gel method is the most widely chosen due to flexible, low temperature, the easy control of ingredients and a low cost for large-scale manufacturing. Literature shows that Yb doping on $\text{Bi}_4\text{Ti}_3\text{O}_{12}$ films by the sol-gel method exhibited high remnant polarization (2Pr) of 58 $\mu\text{C}/\text{cm}^2$ and low coercive field (2Ec) of 116 kV/cm [1], respectively. Ferroelectric $\text{Bi}_{3.25}\text{La}_{0.75}\text{Ti}_3\text{O}_{12}$ (BLT) and $\text{Bi}_{3.15}\text{Nd}_{0.85}\text{Ti}_3\text{O}_{12}$ (BNT) thin films were also made by sol-gel with the remnant polarization (2Pr) and coercive field (2Ec) values of 25.1 $\mu\text{C}/\text{cm}^2$ and 203 kV/cm for BLT, and 44.2 $\mu\text{C}/\text{cm}^2$ and 296 kV/cm for BNT, respectively [7]. Ferroelectric thin films with Dy substitution prepared by sol-gel method exhibited the largest remnant polarization (2Pr) of 53.06 $\mu\text{C}/\text{cm}^2$ after annealing at 710°C [8]. $\text{Bi}_{3.25}\text{La}_{0.75}\text{Ti}_3\text{O}_{12}$ thin films possessed the largest Pr of 17.8 $\mu\text{C}/\text{cm}^2$ with the Ec of 73.6 kV/cm for the film [3].

There is little research with regard to Ce-substituted BTO thin films. Some literature reported optical properties and microstructure of Ce-doped PZT thin films prepared by sol-gel [9], and the preparation and characterization of Ce-doped BaTiO_3 thin films fabricated by pulsed laser deposition was also reported [10]. This paper describes the preparation of Ce-substituted thin films on Pt/TiO₂/SiO₂/Si substrates by the sol-gel method. The influences of doping content on structures, and the properties of ferroelectricity [11], especially the influence on phase, residual polarization and coercive electric field were investigated in our research.

2 Materials and methods

Ferroelectric $\text{Bi}_{4-x}\text{Ce}_x\text{Ti}_3\text{O}_{12}$ (BCeT) ($x=0, 0.2, 0.4, 0.6, 0.8$) thin films were deposited on Pt/Ti/SiO₂/Si substrates by sol-gel processes at 700°C. $\text{Bi}(\text{NO}_3)_3 \cdot 5\text{H}_2\text{O}$, $\text{Ti}(\text{OC}_4\text{H}_9)_4$, $\text{Ce}(\text{NO}_3)_2 \cdot 6\text{H}_2\text{O}$ were selected as starting materials. $\text{Bi}(\text{NO}_3)_3 \cdot 5\text{H}_2\text{O}$ and $\text{Ce}(\text{NO}_3)_2 \cdot 6\text{H}_2\text{O}$ were first dissolved in ethylene glycol monomethyl ether solution at room temperature with constant stirring for 30 min. An excess of 10 mol% Bi was added to the solution, aimed at minimizing the bismuth loss during annealing. $\text{Ti}(\text{OC}_4\text{H}_9)_4$ 5.2 ml mixed with ethylene glycol monomethyl ether and acetylacetone 10 ml during constant stirring at room temperature for 15 min, then solution B was slowly added to solution A at the speed of one drop every second. The two solutions were mixed with constant stirring at room temperature for

1 h. The final content of BCeT in the end solution was 0.1 mol/l. The solution was spin-coated on Pt/TiO₂/SiO₂/Si substrates at 4000 r/min for 20 s. The gel film was dried at 150°C for 15 min on a hot plate and afterwards annealed at 400°C for 10 min, and hereafter the films were annealed at 700°C for 1 h in room temperature. We repeated the above process five times to obtain the final film with a thickness of about 500 nm. Crystalline orientation, lattice parameter and phase of the films were measured by XRD (D8 Advance Bruker AXS, Berlin, Germany) with CuK α radiation. The surface morphologies and microstructures of the sample were observed by FE-SEM (Hitachi Field emission scanning electron microscope SU8010, Tokyo, Japan), ferroelectric hysteresis loop was obtained using a ferroelectric tester (Aix ACCT TF analyzer 1000 Ferroelectric analyzer, Munich, Germany).

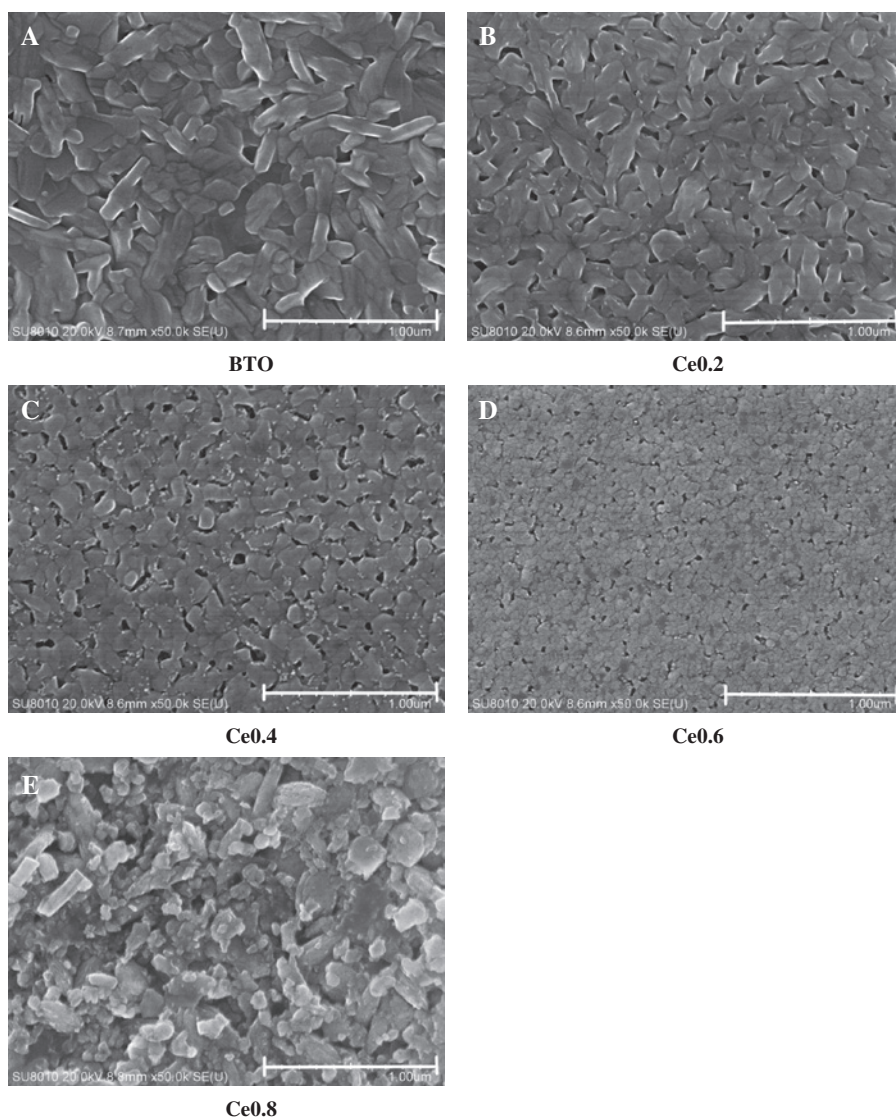


Figure 1 FE-SEM images of BCeT films sample annealed at 700°C.

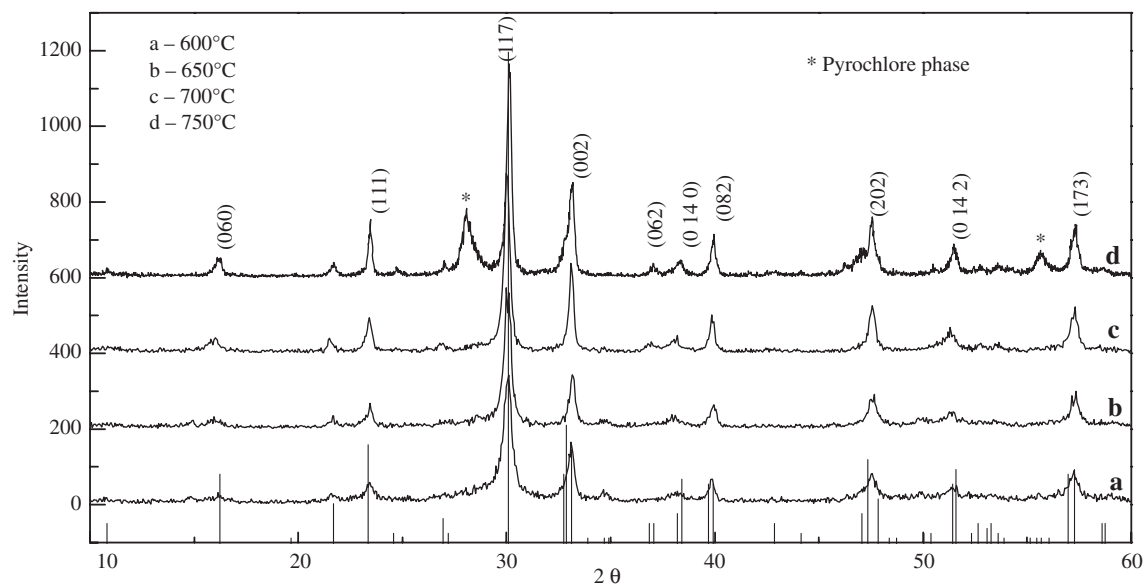


Figure 2 XRD of the powders annealed at different temperatures of 600°C, 650°C, 700°C and 750°C for BceT.

3 Results and discussion

3.1 FE-SEM images of BCeT films sample

The content of Ce had an effect on fracture morphology of BCeT, and FE-SEM images of BCeT films sample test at room temperature are shown in Figure 1. X value in BCeT were 0 and 0.2, corresponding to random orientation [12], with the rare earth element mixing, the grain size became smaller; plate-like grains found with the x value in BCeT was 0.4 [13], corresponded to c-orientation; dot-like grains found with the x value in BCeT was 0.6, that corresponded to a-orientation [14]. It was clearly seen that the grain size

became smaller and the interspace between the grains became smaller too. Because of the distortion caused by the doping rare earth element, the grain growth was inhibited. With the x value in BCe was 0.8, the grain distribution was inhomogenous. The grain size was not regular, for example, rod-like grains, plate-like grains and dot-like grains were all present.

3.2 The XRD patterns of the BCeT powders

Figure 2 shows the XRD patterns of BCeT powders annealed at 600°C, 650°C, 700°C, 750°C for 1 h, respectively. The films with randomly oriented pure bi-layered perovskite-type

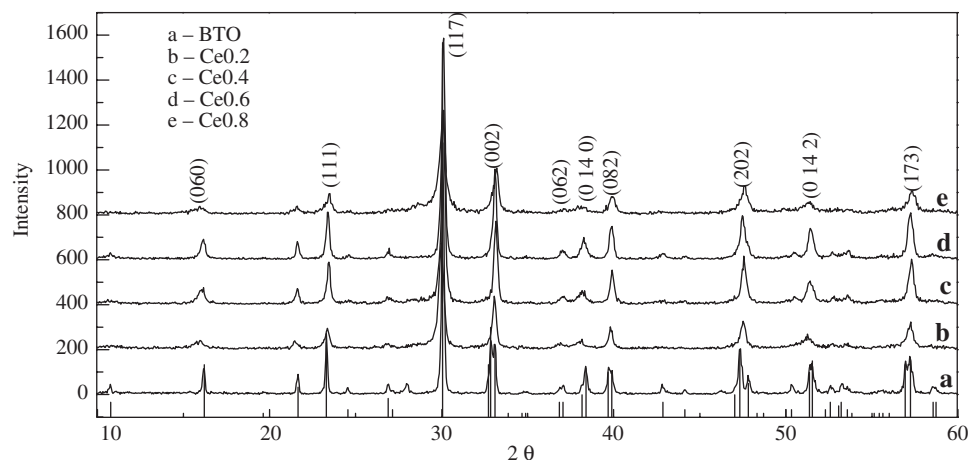


Figure 3 XRD of powders with different Ce contents annealed at 700°C.

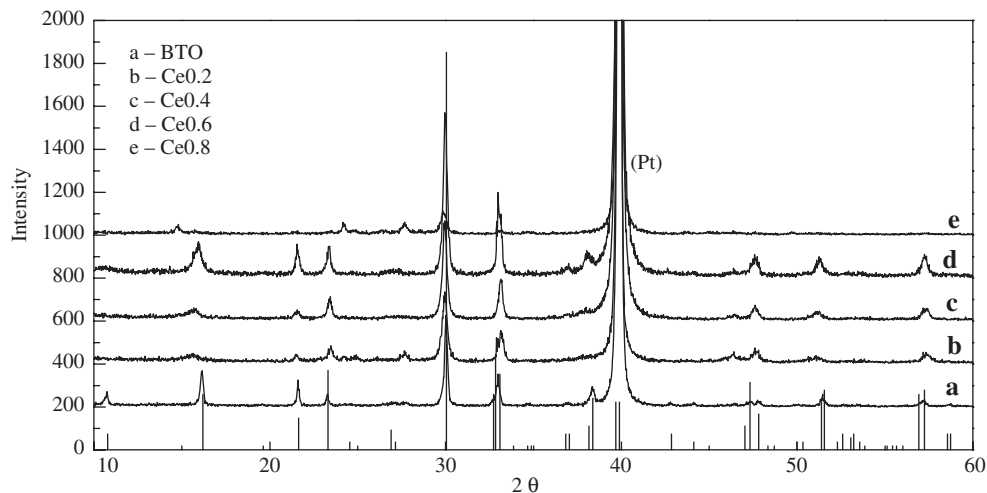


Figure 4 XRD of different Ce contents films on Pt/TiO₂/SiO₂/Si annealed at 700°C.

structure were obtained except at 750°C, the secondary phase named pyrochlore appeared when the annealing temperature was raised to 750°C, which was a by-product when the bismuth amount was less in the formation of BTO. It is evident that with the increase of annealing temperature the diffraction peak intensities increase. We could see when the annealing temperature reached 600°C (117) the diffraction became obvious, which meant the crystallization was in the initial stage; other peaks such as (060) diffraction peaks were not evident, which indicated that there was incomplete crystallization. The diffraction peaks became increasingly sharper with increase of annealing temperature, at the peak width decreased by half and the degree of crystallization was larger.

Figure 3 shows that the XRD of BCeT powders with different Ce contents annealed at 700°C for 1 h, respectively. It was observed that the BCeT had crystallized when the

annealing temperature was 700°C. It also showed that there is no secondary phase formation and the bismuth-layered perovskite structure was formed. The intensity of phase peaks increased as the Ce contents increased. It was evident that the peak became sharper and stronger. Nonetheless, when with the x value was 0.8 the peak intensities became wider and weaker, therefore we could draw a conclusion that the maximum Ce contents was 0.6. An author [15] reported that with a-axis Pr is 50 $\mu\text{C}/\text{cm}^2$ and Ec is 50 kV/cm, and c-axis Pr is 4 $\mu\text{C}/\text{cm}^2$ and Ec is 60 kV/cm, this illustrated that a-axes have a greater contribution to Pr and less to Ec. The (117) diffraction peak was the sharpest and strongest among all of the diffraction peaks. We are eager to get a best a-axis oriented powder, achieved when the x value is 0.6.

XRD patterns of different Ce contents films on Pt/TiO₂/SiO₂/Si annealed at 700°C for 1 h are shown in Figure 4.

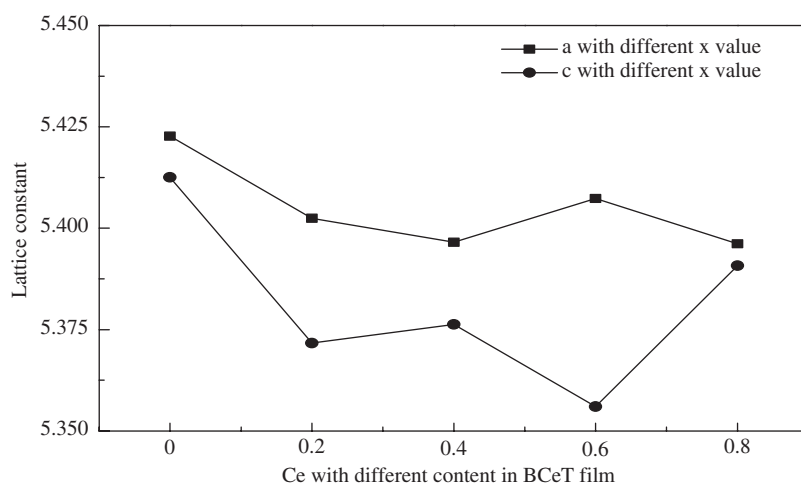


Figure 5 The lattice parameter with different Ce contents annealed at 700°C.

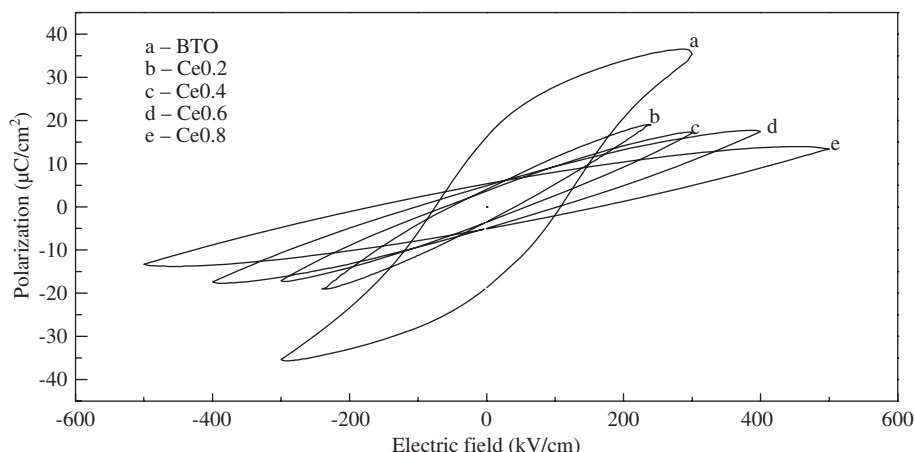


Figure 6 P-E hysteresis loops of different Ce contents annealed at 700°C.

The (117) diffraction peak is the most strongest, which is consistent with the bismuth-layered perovskite structure and without any secondary phase. The diffraction peak intensity became stronger and obvious when the x value was increased. When the x value in BCeT was 0.6, the peak was the strongest and sharpest. When the x value in BCeT was 0.8, the diffraction peak was not obvious, when the content is less than the x value in BCeT was 0.8, the diffraction peak started to become obvious, but the intensity was weak except when the x value is 0.6.

As shown in Figure 5, we could clearly see the variation around the lattice parameters a and c with different Ce contents annealed at 700°C, and the lattice parameter was reduced at first with the increase of doping content, but when the doping contents reached 0.6, the lattice parameter became larger, then dropped with added doping. The lattice parameter c reduced first with the increase of doping content up to an x value in BCeT of

0.2. Compared with the doping amount of 0.2 when the doping amount of the x value in BCeT was 0.4, the lattice parameter c increased and then decreased significantly, when the x value in BCeT of 0.8 became much larger. The x value in BCeT of 0.6 was a turning point which had the bigger a and the least c lattice parameter that confirmed the conclusion in Figure 3.

3.3 The ferroelectric properties of the BCeT

As shown in Figure 6, it was the electric hysteresis loop (P-E loop) that we tested with different Ce doping content of BCeT film, it seemed that they were able to be saturated. With the increase of the doping content, the remaining polarization value was decreased, this was because bismuth loss in the process of heating and formation of oxygen vacancies, the presence of oxygen vacancy on

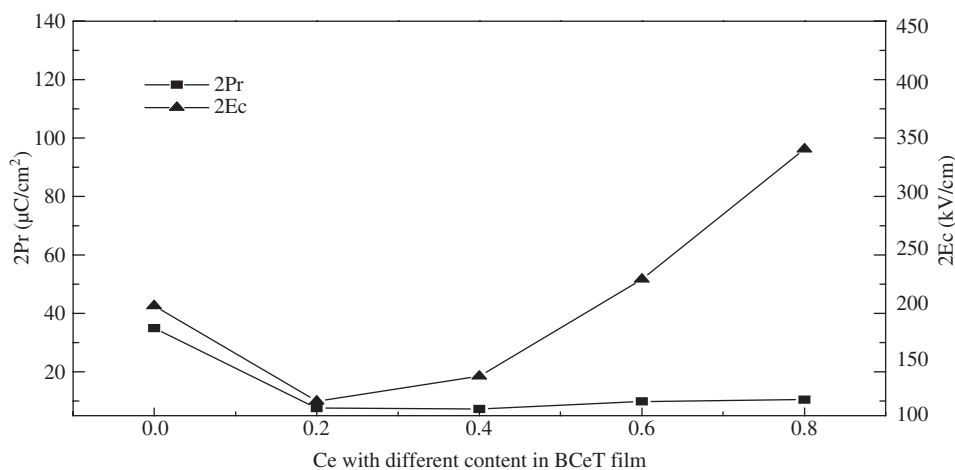


Figure 7 Pr and Ec of different Ce contents.

the turn of ferroelectric, electric domain produce intense pinning effect, which can reduce the ferroelectric property about film [16]. Oxygen vacancy emerges too quickly for Bi evaporation, and rare earth atoms cannot catch up with the reduction of oxygen vacancy, but when the x value in BCeT of 0.6, remaining polarization value increased noticeably. Coercive electric field along with the increase of doping content decreased initially, and then began to increase when the Ce content reached 0.6. This was due to the Ce doping in BTO film replacing the Bi, which reduced the formation of oxygen vacancies, the change of the valence state of the Ce reduced the distortion.

In order to show the influence of the doping content on the electric properties, Figure 7 shows the remanent polarization values and the coercive field values dependent on Ce content in BCeT film. It showed that the remanent polarization values decreased with the increase of the doping content initially, and then increased. The coercive field values decreased with the increase of the doping content initially, and then increased also. Obviously, a small amount of Ce doping can improve the electric properties of BTO. It maybe due to the ferroelectric thin BTO film led to anisotropy, and its electric performance was close to the orientation of film. This meant that the Pr of BCeT film was mainly dependent on (117) orientation and crystal growth. A small amount of the Ce doping made the BTO film had a certain degree of lattice distortion. With

oxygen space increased, the lattice constant decreased and the crystal growth was inhibited. Along with the increase of the content of the Ce ions into the $(\text{Bi}_2\text{O}_3)^{2+}$ layer, Ti valencies were many and various, which lead to decline of ferroelectric thin film [17]. When Ce doping content continued to increase, the Ce still existed in the form of Ce^{3+} , and the lattice distortion of BCeT film began to reduce. The remanent polarization values (2Pr) and coercive field values (2Ec) of 0.6 Ce-substituted BCeT films were $9.86 \mu\text{C}/\text{cm}^2$ and $208 \text{ kV}/\text{cm}$, respectively.

4 Conclusions

Single phase of bi-layered perovskite BCeT ($x=0, 0.2, 0.4, 0.6$ and 0.8) thin films were prepared by sol-gel method. The best temperature of crystallization of BCeT films was 700°C and the final film thickness was 500 nm . With the x value of 0.6 the films diffraction peak was sharpest and strongest and no impurity peaks formed. The remanent polarization values (2Pr) and coercive field values (2Ec) of 0.6 Ce-substituted films were $9.86 \mu\text{C}/\text{cm}^2$ and $208 \text{ kV}/\text{cm}$, respectively.

Received December 8, 2013; accepted March 19, 2014; previously published online April 10, 2014

References

- [1] Kao MC, Chen HZ, Young SL. *Mater. Lett.* 2008, 62, 3243–3245.
- [2] Kang SW, Rhee SW. *J. Mater. Sci.* 2004, 15, 231.
- [3] Li JJ, Li P, Zhang GJ, Yu J. *J. Mater. Sci. Mater. Electron.* 2011, 22, 299–303.
- [4] Kuo DH, Chiang KC. *Solid Films* 2008, 516, 5985–5990.
- [5] Simões AZ, Ries A, Stojanovic BD, Biasotto G, Longo E, Varela JA. *Ceram. Int.* 2007, 33, 1535–1541.
- [6] Chia WK, Chen YC, Yang CF, Tzou WC. *J. Phys. Chem. Solids* 2008, 69, 465–469.
- [7] Li MY, Pei L, Liu J, Yu BF, Guo DY, Sun XH, Zhao XZ. *Sci. China Ser. E. Tech. Sci.* 2008, 51, 1843–1849.
- [8] Cheng CP, Tang MH, Ye Z, Zhou YH, Zheng XJ, Hu ZS, Hu HP. *Mater. Lett.* 2007, 61, 4117–4120.
- [9] Guo DY, Li MY, Liu J, Yu BF, Pei L, Wang YB, Yu J, Yang B. *Sci. China Ser. E. Tech. Sci.* 2008, 51, 10–15.
- [10] Cernea M, Ianculescu A, Monnereau O, Bley V, Bastide B, Logofatu C. *J. Mater. Sci.* 2004, 39, 2755–2759.
- [11] Zhong XL, Hu ZS, Li B, Wang JB, Liao H, Zhou YC. *J. Cryst. Growth* 2008, 310, 4516–4520.
- [12] Lee HN, Hesse D. *Appl. Phys. Lett.* 2002, 80, 1040–1043.
- [13] Hiroshi U, Hiroki Y, Isao O, Hirofumi M, Tekashi W, Takayuki W, Takashi K, Hiroshi F. *Appl. Phys. Lett.* 2002, 81, 2229–2231.
- [14] Lee HN, Hesse D, Zakharov N, Göosele U. *Science* 2002, 296, 2006–2009.
- [15] Cummins SE, Cross LE. *J. Appl. Phys.* 1968, 39, 2268–2274.
- [16] Feng X, Wang H. *J. Chinese Ceram. Soc.* 2010, 38, 1026–1030.
- [17] Girault C, Damiani D, Aubreton J, Catherinot A. *Appl. Phys. Lett.* 1989, 55, 182.